

# Biodiesel synthesis from *Ceiba pentandra* oil by microwave irradiation-assisted transesterification: ELM modeling and optimization



A.S. Silitonga<sup>a,\*</sup>, A.H. Shamsuddin<sup>b</sup>, T.M.I. Mahlia<sup>c</sup>, Jassinne Milano<sup>d,\*\*</sup>, F. Kusumo<sup>e</sup>,  
Joko Siswanto<sup>f</sup>, S. Dharma<sup>a</sup>, A.H. Sebayang<sup>a</sup>, H.H. Masjuki<sup>d</sup>, Hwai Chyuan Ong<sup>d</sup>

<sup>a</sup> Department of Mechanical Engineering, Politeknik Negeri Medan, 20155, Medan, Indonesia

<sup>b</sup> Institute of Sustainable Energy, Universiti Tenaga Nasional, 43000, Kajang, Selangor, Malaysia

<sup>c</sup> School of Systems, Management and Leadership, Faculty of Engineering and Information Technology, University of Technology Sydney, NSW, 2007, Australia

<sup>d</sup> Department of Mechanical Engineering, Faculty of Engineering, University of Malaya, 50603, Kuala Lumpur, Malaysia

<sup>e</sup> Department of Computer Science & Information Technology, College of Computer Science & Information Technology Universiti Tenaga Nasional, 43000, Kajang, Selangor, Malaysia

<sup>f</sup> Department of Informatics Engineering, Faculty of Engineering, Universitas Surabaya, Jl. Kali Rungkut, Surabaya, 60293, Indonesia

## ARTICLE INFO

### Article history:

Received 14 July 2018

Received in revised form

20 June 2019

Accepted 11 July 2019

Available online 12 July 2019

### Keywords:

*Ceiba pentandra* biodiesel

Extreme learning machine

Cuckoo search algorithm

Microwave irradiation-assisted

transesterification

Alternative fuel

## ABSTRACT

In this study, microwave irradiation-assisted transesterification was used to produce *Ceiba pentandra* biodiesel, which accelerates the rate of reaction and temperature within a shorter period. The improvement of biodiesel production requires a reliable model that accurately reflects the effects of input variables on output variables. In this study, an extreme learning machine integrated with cuckoo search algorithm was developed to predict and optimize the process parameters. This model will be useful for virtual experimentations in order to enhance biodiesel research and development. The optimum parameters of the microwave irradiation-assisted transesterification process conditions were obtained as follows: (1) methanol/oil ratio: 60%, (2) potassium hydroxide catalyst concentration: 0.84%(w/w), (3) stirring speed: 800 rpm, and (4) reaction time: 388 s. The corresponding *Ceiba pentandra* biodiesel yield was 96.19%. Three independent experiments were conducted using the optimum process parameters and the average biodiesel yield was found to be 95.42%. In conclusion, microwave irradiation-assisted transesterification is an effective method for biodiesel production because it is more energy-efficient, which will reduce the overall cost of biodiesel production.

© 2019 Elsevier Ltd. All rights reserved.

## 1. Introduction

Biodiesels are promising alternative fuels for petroleum-derived diesel fuels owing to their similarities between the physicochemical properties of biodiesels and those of diesel [1]. Biodiesels are non-toxic and environmentally friendly with lower carbon dioxide (CO<sub>2</sub>), carbon monoxide (CO), and nitrogen oxide (NO<sub>x</sub>) emissions compared with petroleum-derived diesel. The higher flash points of biodiesels facilitate in their storage and transportation [2].

There is growing interest in biodiesel production worldwide

because of its eco-friendliness and additionally, biodiesels can be produced from renewable sources. Biodiesels have higher flash points, rendering these fuels safer alternatives for handling and transportation compared with diesel [3]. Biodiesels also have more favorable combustion, engine performance, and exhaust emission characteristics compared with diesel including lower CO, particulate matter (PM), and unburned hydrocarbons (UHC) [4]. The escalating increase in energy demands due to industrialization has led to a significant increase in the imports of crude oils in developing countries.

Computational tools are commonly used to analyze and/or design complex systems [5]. Modeling has gained popularity because of its flexibility and its ability to simulate and analyze real-world systems in detail. Hence, modeling can be used as a supporting tool to complement experimental techniques. Simulation models require fewer restrictive assumptions to represent complex

\* Corresponding author. Department of Mechanical Engineering, Politeknik Negeri Medan, 20155, Medan, North Sumatra, Indonesia.;

\*\* Corresponding author.;

E-mail addresses: [arridina@polmed.ac.id](mailto:arridina@polmed.ac.id), [ardinsu@yahoo.co.id](mailto:ardinsu@yahoo.co.id) (A.S. Silitonga), [jassinneemilano@hotmail.com](mailto:jassinneemilano@hotmail.com), [jassinneemilano.jm@gmail.com](mailto:jassinneemilano.jm@gmail.com) (J. Milano).

dynamic systems and fairly complex models can be developed with relatively high dimensionality [6]. Hence, modeling is essentially a trial-and-error process, in which a set of inputs is used to predict a set of outputs. A good system design is attained once the desired performance is achieved. The simulation process is repeated until a satisfactory set of performance measures is obtained.

Many studies have examined the use of traditional artificial neural networks (ANNs), which are well-known types of evolutionary computational methods and which have gained popularity over the last few decades. Several ANN topologies have been used to optimize biodiesel production processes (esterification and transesterification reactions) as well as to improve the physico-chemical properties, engine performance, and exhaust emission characteristics of biodiesels [7,8]. The efficiency of ANNs in modeling bioprocesses has been reported in several studies [9–11]. However, there are many drawbacks with conventional ANNs owing to their limitations in learning process, such as the existence of multiple local minima, slow learning speed, large training data size, and poor generalization performance. In addition, the users need to determine the optimal ANN architecture.

Extreme learning machine (ELM) is a mathematical modeling approach that can be used to solve the aforementioned problems [10,12]. The ELM is a single-hidden-layer feedforward ANN where the parameters of the hidden layer are initialized randomly. Moreover, ELM can calculate the output weights analytically using the Moore–Penrose generalized inverse. For this reason, ELM is advantageous because of its speed and better generalization capability compared with conventional ANNs [12,13]. Sebayang et al. [14] used ELM to predict the engine performance and exhaust emission characteristics of *Manihot glaziovii* bioethanol-gasoline blends. The results showed the coefficient of determination ( $R^2$ ) is close to 1 and the mean absolute percentage error (MAPE) is less than 3% for all parameters. The results indicate the ELM model is capable of predicting the engine performance and exhaust emissions of bioethanol-gasoline fuel blends.

Wong et al. [15] compared three mathematical models (ELM, least-squares support vector machine, and radial basis function neural network) to determine the optimal biodiesel ratio that can reduce exhaust emissions within the engine operation range. The results showed the mean absolute percentage errors for the test data sets ( $MAPE_{test}$ ) were 2.06 and 34.74% whereas the root mean square percentage errors for the test data sets ( $RMSPE_{test}$ ) were 0.29 and 28.01%. This indicates that ELM, as one of the potential modeling techniques, is the best modeling technique for optimization purposes because of its high accuracy and accelerated modeling time. Therefore, ELM modeling has been used to predict the engine performance and exhaust emission characteristics of biodiesels. Kusumo et al. [7] compared kernel-based extreme learning machine (K-ELM) and ANN models for *Ceiba pentandra* biodiesel production. The results showed the K-ELM provided more reliable predictions compared with the ANN model.

### 1.1. Microwave irradiation-assisted transesterification

Biodiesel can be produced by conventional heating, enzymatic catalysis, supercritical methanol, and microwave irradiation-assisted transesterification [16–18]. Microwave irradiation-assisted transesterification is more energy-efficient owing to the direct transfer of energy to the reactants through microwave radiation, which eliminates the need for preheating. In recent years, microwave reactors have been used to convert triglycerides in oils into biodiesels because of their high product selectivity, significant energy savings, and accelerated transesterification reaction compared with conventional heating systems [19–21]. Transesterification reaction involves transforming triglycerides in oils or

fats into fatty acid alkyl esters in the presence of an alcohol (e.g., methanol or ethanol) and catalyst, producing glycerol as a by-product [22,23]. The cost of biodiesel production is related to the cost of raw materials (production and processing), catalysts, biodiesel processing (energy, consumables and labor), transportation (raw materials and final products), as well as local and national taxes [24]. To date, crude oils are primarily used as feedstocks in most biodiesel plants, where the cost of vegetable oils accounts for nearly 80% of the overall biodiesel production cost [1,17,18]. Microwave reactors have been used in transesterification reactions, and microwave irradiation-assisted transesterification has been accepted as a suitable method to separate and purify thermo-sensitive compounds with high molecular weights [19,25,26]. This is possible owing to the small distance between the condenser and chamber, which is in the order of the mean free path of the evaporating molecules. Microwave reactors are better than conventional reactors as they can be used to increase biodiesel production and attain higher production capacities [18,27,28]. A simple and robust design of tubular reactors with static mixers in the microwave reactors can overcome the shortcomings of conventional heating reactors by efficiently increasing the mass transfer rate between the phases without the need for moving parts, which reduces investment, operation, and maintenance costs [29,30]. The objective of this study was to optimize the parameters of microwave irradiation-assisted transesterification to produce *Ceiba pentandra* biodiesel by using ELM coupled with cuckoo search (CS) algorithm.

## 2. Materials and methods

### 2.1. Materials and reagents

Crude *Ceiba pentandra* oil was sourced from Kebumen, Central Java, Indonesia, which has about 23 million tons of *Ceiba Pentandra* stalks with an average production of 3 tons per hectare. The average oil seed yield is 1280 kg/ha. *Ceiba Pentandra* seeds have about 25–28%(w/w) of oil in each fruit [31]. In this study, crude *Ceiba pentandra* oil (CCPO) was extracted using a screw extruder machine. However, to increase the yield of CCPO, the seeds were repeatedly pressed using a manual hydraulic pressing machine.

Oxidation stability is one of the parameters used to assess the quality of a fuel. Oxidation stability indicates the degree of oxidation and the potential reactivity of a fuel with air. This parameter can be used to determine if antioxidants are needed. Oxidation occurs due to the presence of unsaturated fatty acid chains and double bonds in the parent molecules, which immediately react with the oxygen as soon as the fuel is exposed to air [32]. The chemical composition of crude oils render these oils more susceptible to oxidative degradation compared with diesel [33]. The Rancimat method is used to measure the oxidative stability of fuels

**Table 1**  
Fatty acid composition of the CCPO.

Fatty acid	Composition %(w/w)
C12:0 (Lauric acid)	0.1
C14:0 (Myristic acid)	0.1
C16:0 (Palmitic acid)	20.8
C16:1 (Palmitoleic acid)	0.5
C18:0 (Stearic acid)	4.2
C18:1 (Oleic acid)	17.0
C18:2 (Linoleic acid)	38.2
C18:3 (Linolenic acid)	1.3
C20:0 (Arachidic acid)	0.8
18:°CE (Malvalic acid)	16.8

<sup>a</sup> CE: Cyclopropane ester.

in the ASTM D6751 and EN 14214 standard methods. Based on the fatty acid composition of the CCPO shown in Table 1, it can be expected the *Ceiba pentandra* biodiesel will have good oxidation stability. Proper handling and preventing the crude oil from exposure to air and sunlight during the storage period will help prolong the oxidation stability of the oil. The CCPO needs to be transesterified into biodiesel for it to be used in compression ignition engines.

The following reagents were used for biodiesel production: (1) methanol (purity: 99.9%, American Chemical Society-grade reagent), sulfuric acid (purity: >98.9%), ortho-phosphoric acid (purity: 85%), anhydrous sodium sulfate (purity: 99%), sodium hydrogen carbonate, and potassium hydroxide pellets (purity: 99%).

## 2.2. Instruments and apparatus

The physicochemical properties of the biodiesel (kinematic viscosity, density, flash point, cloud point, pour point, higher heating value, acid value, oxidation stability, and copper strip corrosion) were measured according to the ASTM D445, ASTM D127, ASTM D93, ASTM D2500, ASTM D240, ASTM D664, EN 14112, and ASTM D130 standard test methods respectively. Agilent 7890A gas chromatograph system equipped with a flame ionization detector (FID) was used to determine the fatty acid methyl ester (FAME) content of the biodiesels. HP Innowax column (length  $\times$  inner diameter  $\times$  film thickness: 30 m  $\times$  0.25 mm  $\times$  0.25  $\mu$ m) was used for FAME measurements. A gas chromatograph system equipped with an FID and cool on-column injector was used to measure the glycerol and glyceride content of the biodiesels according to the EN 14105:2011 standard. Agilent VF-5ht Ultimetall (length  $\times$  inner diameter  $\times$  film thickness: 15 m  $\times$  0.32 mm  $\times$  0.1  $\mu$ m) was used for glycerol and glyceride testing. The resulting mixture was immediately analyzed using Fourier transform infrared (FTIR) spectrometer (Model: TENSOR 27, Bruker, USA). Each experiment was conducted in triplicate and the data was expressed in terms of mean and standard deviation.

## 2.3. Microwave reactor

Anton Paar Monowave 400 microwave reactor with Autosampler MAS 24 was used in this study. This reactor was equipped with infrared sensors for precise temperature control and pressure sensors in order to monitor the reaction in the closed vessel. The built-in magnetic stirrer provides adequate stirring in order to attain a homogeneous mixture, as shown in Figs. 1 and 2. The Monowave 400 microwave reactor chamber has three stages: (1) the closed vessel was heated to the desired temperature, (2) the temperature was maintained at the set temperature over a specific time, and (3) the closed vessel was cooled to the desired temperature in order to terminate the transesterification reaction. During the reaction, the power output was controlled based on the set temperature for the experiment. The power output is automatically controlled to prevent the reaction from becoming exothermic during the transesterification reaction. The technical specifications of the Anton Paar Monowave 400 microwave reactor with Autosampler MAS 24 are shown in Table 2. The microwave irradiation produced goes through the glass reaction vessel wall and directly heats up the reaction mixture. The conversion of electromagnetic energy into heat energy is highly efficient, resulting in extremely fast heating rates within minutes. The microwave irradiation provides energy to the molecules such that the molecules stretch and rotate, resulting in energy activation. The rapid heating to the set temperature and immediate cooling after the conversion process suppresses the formation of by-products.



Fig. 1. Anton Paar Monowave 400 microwave reactor.

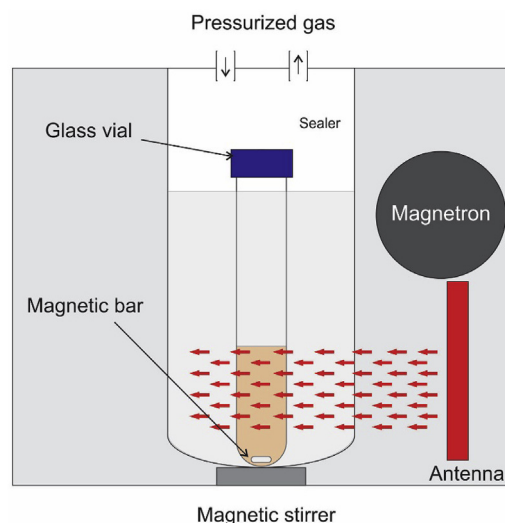


Fig. 2. Schematic of the experimental setup using the Anton Paar Monowave 400 microwave reactor.

**Table 2**  
Technical specifications of the Anton Paar Monowave 400 microwave reactor.

Parameters	Monowave 400
Maximum filling volume	20 mL for a 30-mL vial
Maximum operation pressure	30 bars (435 psi)
Maximum infrared temperature	300 °C
Maximum fiber-optic temperature	300 °C
Maximum power	850 W
Vial material	Borosilicate glass
Cap material	Polyether ether ketone (PEEK)
Camera	Integrated
Autosampler MAS24	Yes
Seal material	Teflon-coated silicone

## 2.4. Esterification process

It was necessary to pretreat the CCPO in order to reduce its free

fatty acid content and acid value prior to the transesterification process. Acid-catalyzed esterification was used for this purpose, where sulfuric acid ( $H_2SO_4$ ) was chosen as the catalyst. The following parameters were used for the acid-catalyzed esterification process: (1) methanol: 40%(v/v), (2)  $H_2SO_4$  concentration: 1.8%(v/v), and (3) stirring speed: 800 rpm. These values were chosen based on the work of Kusumo et al. [7]. The esterification process was assisted by microwave irradiation using the microwave reactor. The reaction time for the esterification process was varied at 120, 180, 240, 300, and 360 s while the reaction temperature was fixed at 100 °C [34]. After the esterification process, the reaction mixture was left to settle under gravity in a separating funnel for 2 h. The by-products and catalyst were removed after the esterification process and the product was washed with warm deionized water (20% of the volume of the products) at 40 °C in order to remove impurities. The methanol and water residues were evaporated from the esterified oil using a rotary evaporator under vacuum.

### 2.5. Transesterification process

Anton Paar Monowave 400 high-performance microwave reactor with Autosampler MAS24 was used for the microwave irradiation-assisted transesterification, where the esterified oil was converted into *Ceiba pentandra* methyl ester (CPME). The steps involved in the production of CPME from the esterified *Ceiba*

*pentandra* oil by microwave irradiation-assisted transesterification are summarized in the form of a flow chart (see Fig. 3).

Box-Behnken design was used for the experimental design. Four parameters were chosen for this study: (1) stirring speed (600, 750, 900 rpm), (2) reaction time (240, 360, 480 s), (3) potassium hydroxide (KOH) catalyst concentration (0.6, 0.8, 1.0%(w/w)), and (4) methanol/oil ratio (50, 60, 70%). The total number of experimental runs was 29. The Box-Behnken experimental design for the microwave irradiation-assisted transesterification process is shown in Table 3. The operating conditions followed Milano et al. [34], Jermolovicus et al. [35], and El Sherbiny et al. [36], who conducted optimization studies of biodiesel production from edible and non-edible oils using microwave irradiation-assisted method. Milano et al. [34] recommended: (1) methanol/oil ratio: 59.60%, (2) catalyst concentration: 0.77%, (3) stirring speed: 600 rpm, and (4) reaction time: 429 s, while Jermolovicus et al. [35] suggested reaction time can be completed at 450 s with 1.76 W/g of microwave power and lastly Sherbiny et al. [36] recommended (1) methanol/oil molar ratio: 7.5:1 (approximately methanol/oil ratio:35%), (2) reaction time: 120 s, (3) catalyst concentration: 1.5%. The methyl ester yield obtained from the transesterification process was based on the following equation:

$$\text{Methyl ester yield (\%)} = \frac{M_{ME}}{M_O} \times 100 \quad (1)$$

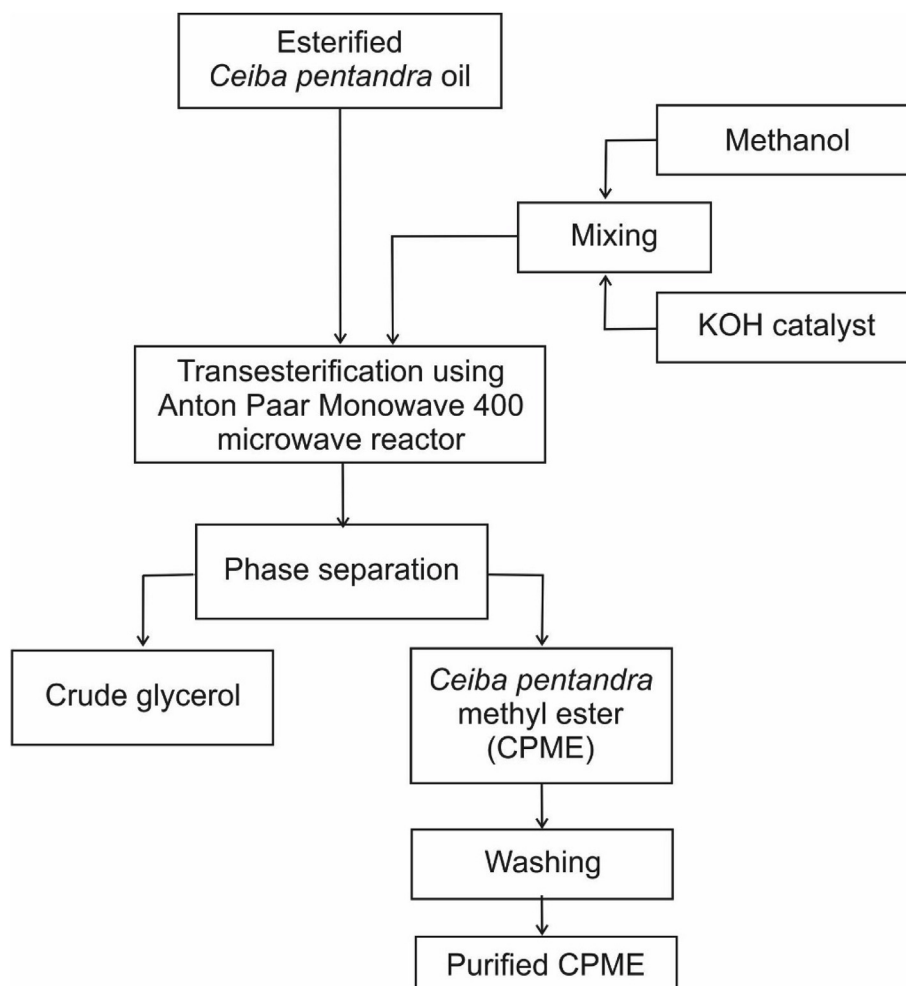


Fig. 3. Steps involved in microwave irradiation-assisted transesterification process of esterified *Ceiba Pentandra* oil.

**Table 3**  
Box-Behnken experimental design for the microwave irradiation-assisted transesterification process.

Run	Stirring speed (rpm)	Reaction time (s)	KOH catalyst concentration (%(w/w))	Methanol/oil ratio (%)	<i>Ceiba pentandra</i> methyl ester yield from Box-Behnken experiment (%)	<i>Ceiba pentandra</i> methyl ester yield from ELM prediction (%)
1	750	240	0.8	50	75.99	76.00
2	750	360	0.8	60	93.25	94.62
3	900	360	1.0	60	89.77	89.77
4	750	240	0.6	60	71.25	71.28
5	750	240	0.8	70	79.17	80.58
6	600	360	0.8	50	79.14	81.21
7	750	360	1.0	70	84.91	84.92
8	900	480	0.8	60	90.22	90.21
9	750	480	0.6	60	75.18	75.24
10	750	360	1.0	50	89.00	87.46
11	750	360	0.8	60	94.42	94.62
12	600	360	0.6	60	75.64	75.64
13	600	480	0.8	60	83.21	83.21
14	900	360	0.8	70	91.33	91.32
15	600	360	1.0	60	85.05	85.04
16	600	240	0.8	60	75.53	75.53
17	750	360	0.8	60	94.99	94.62
18	600	360	0.8	70	86.11	86.10
19	750	240	1.0	60	77.27	77.32
20	900	360	0.8	50	89.27	89.26
21	750	360	0.8	60	94.19	94.62
22	750	480	0.8	50	86.46	86.46
23	750	360	0.8	60	94.39	94.62
24	900	360	0.6	60	81.97	81.92
25	750	360	0.6	50	74.63	74.63
26	750	360	0.6	70	83.41	83.41
27	750	480	0.8	70	89.16	89.16
28	750	480	1.0	60	87.02	87.06
29	900	240	0.8	60	81.79	81.79
R <sup>2</sup>					0.992	
RMSE					0.142	

where  $M_{ME}$  is the weight of the methyl ester produced in grams (g), and  $M_O$  is the weight of the esterified *Ceiba pentandra* oil in grams (g).

The number of experimental runs ( $N$ ) required for the Box-Behnken experimental design was based on the following equation:

$$N = 2k(k - 1) + N_c \quad (2)$$

where  $k$  is the number of factors and  $N_c$  is the number of central points [37].

## 2.6. ELM model

The efficacy of ELM model is dependent on input data and therefore, it is crucial to scale the input and output data. In this study, the experimental input and output data were normalized using a simple normalization method [15]. The training model dataset was normalized using the following equation [7]:

$$N_i = \frac{x_i - m}{s} \quad (3)$$

where  $N_i$  represents the normalized parameter,  $x_i$  is the original variable, and  $m$  and  $s$  represent the mean and standard deviation of  $x_i$  respectively.

Since all of the values in the training process were normalized, the values predicted by the models needed to be denormalized using the inverse of Eq. (1). The data was normalized within a range of 0.1–0.9 [14]. After normalization, the data were randomized before training.

The ELM was initially developed for single-hidden-layer feed-forward networks (SLFNs). The SLFNs are widely used to approximate complex nonlinear mappings directly from the input samples

where the parameters of the hidden layer in ELM are initialized randomly. Output weights were calculated using Moore-Penrose generalized inverse. The output function of the ELM for generalized SLFNs is expressed as [15,38]:

$$f_L(x) = \sum_{i=1}^L \beta_i G(w_i, b_i, x), \quad x \in R^n, \quad a_i \in R^n \quad (4)$$

where  $w_i$  and  $b_i$  are the learning parameters of the hidden nodes,  $\beta_i$  is the weight that connects the  $i$ th hidden node and the output node. The function  $G(w_i, b_i, x)$  shows the output value of the  $i$ th hidden node for the input  $x$ . The additive hidden node with the activation function  $g(x) : R \rightarrow R$  (e.g., sigmoid and threshold) is expressed as:

$$G(w_i, b_i, x) = g\left(\sum_{j=1}^n w_{ij}x_j + b_i\right), \quad b_i \in R \quad (5)$$

where  $w_{ij} = [w_{i1}, w_{i2}, \dots, w_{in}]^T$  is the weight vector that connects the input layer and  $i$  is the hidden node  $i$  with input to  $j$ ,  $b_i$  is the bias of the  $i$ th hidden node and  $a_i, x = [x_1, x_2, \dots, x_n]^T$  is the inner product of vector  $a_i$  in  $R^n$ .

By using Eq. (3), one can determine  $G(w_{ij}, b_i, X)$  for the radial basis function (RBF) hidden node with the activation function  $g(x) : R \rightarrow R$  (e.g., Gaussian) given in Eq. (4) as follows [39]:

$$G(w_i, b_i, x) = g\left(b_i \sqrt{\sum_{j=1}^n (x_j - w_{ij})^2}\right)^T, \quad b \in R^+ \quad (6)$$

Here,  $w_i$  and  $b_i$  represent the center and impact factor of  $i$ th RBF node,  $R^+$  represents the set of all positive real values. An RBF

network forms if the SLFN has RBF nodes in its hidden layer. For  $N$ , the arbitrary distinct sample is  $(x_i, t_i) \in R^n \times R^m$  where the  $n \times 1$  input vector is represented by  $x_i$  and the  $m \times 1$  target vector is represented by  $t_i$ . If an SLFN with  $L$  hidden nodes approximate  $N$  samples with zero error, this implies that  $\beta_i$ ,  $w_i$  and  $b_i$  exist such that:

$$f_i(x) = \sum_{i=1}^L \beta_i G(w_i, b_i, x), \quad j = 1, \dots, N \tag{7}$$

Eq. (5) may be expressed compactly as [15]:

$$H\beta = T \tag{8}$$

where

$$H(\tilde{w}, \tilde{b}, \tilde{x}) = \begin{bmatrix} G(w_1, b_1, x_1) & \dots & G(w_L, b_L, x_1) \\ G(w_1, b_1, x_N) & \dots & G(w_L, b_L, x_N) \end{bmatrix}_{N \times L} \tag{9}$$

with  $\tilde{w} = w_1, \dots, w_L$ ;  $\tilde{b} = b_1, \dots, b_L$ ;  $\tilde{x} = x_1, \dots, x_L$ .

$$\beta = \begin{bmatrix} \beta_1^T \\ \vdots \\ \beta_L^T \end{bmatrix}_{L \times m} \quad \text{and} \quad T = \begin{bmatrix} t_1^T \\ \vdots \\ t_L^T \end{bmatrix}_{N \times m} \tag{10}$$

It shall be noted that  $H$  is the hidden layer output matrix of the SLFN, where the  $i$ th column of  $H$  is the output of the  $i$ th hidden node with respect to the inputs  $x_1, \dots, x_n$  in Eq. (7) and (8). Unlike traditional learning algorithms, the ELM tends to cover not only the smallest training error but also the smallest norm of output weights compared with conventional learning algorithms which improves the performance of the regression model. The ELM is based on the idea the parameters of the hidden layer are independent of the training samples and the hidden layer of the generalized SLFNs does not need to be tuned [38].

### 2.7. Cuckoo search algorithm

The CS algorithm consists of three major rules:

- 1) Each cuckoo randomly finds a nest to lay eggs and lays one egg at a time.
- 2) The best nest with high-quality eggs will be carried over to the next generation.
- 3) The number of available host nests is fixed and the host can detect the egg laid by a cuckoo with probability  $p_a \in [0, 1]$ . In this case, the host bird that detects the egg laid by the cuckoo can either throw the egg or build a new nest elsewhere. The last strategy is approximated by the fraction  $p_a$  of the  $n$  nests being replaced by new nests [40,41].

Lévy flight based on the Lévy distribution with infinite mean and variance were used to generate new solutions, i.e.,  $X_i^{(t+1)}$ . This behavior was used to generate new solutions for a cuckoo based on the following equation [42]:

$$X_i^{(t+1)} = X_i^{(t)} + \alpha \hat{Levy}(\lambda) \tag{11}$$

where ( $\alpha > 0$ ) is the step size, which is adjusted according to the scale of the problem of interest.

### 2.8. Random sub-sampling cross validation

Random sub-sampling cross validation was adopted in this

study since the number of datasets (29) used to assess the performance of the ELM model may not be sufficiently large. Random sub-sampling is a multiple holdout based on the idea that the data is randomly split into subsets, where the size of each subset is determined by the user [18,43]. A total of 23 datasets and 6 datasets was used for training and testing respectively. The procedure was repeated ten times and the average absolute deviation (AAD) was determined. The standard deviation (SD) was determined based on Eq (13):

$$AAD = \frac{1}{n} \left( \sum_{i=1}^n \left( \frac{|(y_{ei} - y_{pi})|}{y_{ei}} \right) \right) \tag{12}$$

$$SD = \sqrt{\frac{\sum_{i=1}^n (x_i - \bar{x})^2}{n - 1}} \tag{13}$$

here,  $n$  is the number of experimental data,  $y_{ei}$  is the experimental CPME yield,  $y_{pi}$  is the predicted CPME yield, and  $y_m$  is the average CPME yield determined from experiments. In Eq. (13),  $n$  represents the size of the dataset, and  $\bar{x}$  represents the mean value of the dataset  $x_1, \dots, x_n$ .

### 2.9. Statistical analysis

The performance of the ELM model was assessed based on the coefficient of determination ( $R^2$ ) and root mean square error (RMSE):

$$R^2 = 1 - \sum_{i=1}^n \left( \frac{(y_{ei} - y_{pi})^2}{(y_m - y_{pi})^2} \right) \tag{14}$$

$$RMSE = \sqrt{\frac{1}{n} \sum_{i=1}^n (y_{pi} - y_{ei})^2} \tag{15}$$

where  $n$  is the number of experimental data,  $y_{ei}$  is the experimental CPME yield,  $y_{pi}$  is the predicted CPME yield, and  $y_m$  is the average CPME yield determined from experiments. The accuracy of the model was determined based on the  $R^2$  value and RMSE. The smaller the RMSE and the higher the  $R^2$  value, the higher the accuracy of the model. The  $R^2$  value should not be less than 80% [44].

### 2.10. Sensitivity analysis

Sensitivity analysis is a method employed to determine sensitivity of an outcome (which in this case is the methyl ester conversion yield) to the input parameters. Sensitivity analysis is carried out to determine (1) which parameters require additional research to strengthen the knowledge base, which will reduce output uncertainty, (2) which parameters are insignificant and can be eliminated from the final model, (3) which inputs or parameters have a significant effect that will determine output variability, (4) which parameters are strongly correlated with the output, and (5) once the model is used for production, what are the consequences or results from changing a given input parameter [45]. In this study, Eq. (16) proposed by Garson (1991) was used to measure the level of significance of input variables for CPME, which is based on the partition of weights:

$$pq = \frac{\sum_{r=1}^{M_c} \left( \left( \frac{|W_{qr}^{pc}|}{\sum_{d=1}^{M_p} |W_{dr}^{pc}|} \right) \times |W_{rs}^{cb}| \right)}{\sum_{d=1}^{M_p} \left\{ \sum_{r=1}^{M_c} \left( \frac{|W_{dr}^{pc}|}{\sum_{d=1}^{M_p} |W_{dr}^{pc}|} \right) \times |W_{rs}^{cb}| \right\}} \quad (16)$$

where  $pq$  is the relative significance of the  $qc$  input variable on the output variable,  $M_p$  and  $M_c$  represent the number of input neurons and hidden neurons respectively, and  $W$  represents the connection weights. It shall be noted that the superscripts  $p$ ,  $b$ , and  $c$  represent the input, output and hidden layers respectively, whereas the subscripts  $d$ ,  $s$ , and  $r$  represent the input, output and hidden neurons respectively.

### 2.11. Fuel properties

The physicochemical properties of the CPME produced by microwave irradiation-assisted transesterification using the optimum process parameters were measured. The physicochemical properties (kinematic viscosity, density, acid value, heating value, oxidation stability, flash point, pour point, cloud point, and copper strip corrosion) were determined according to ASTM D6751 and EN 14214 standard test methods and they (the properties) were compared with those for diesel. The FAME content was measured by referring to the EN 14103:2011 standard test method. The FAME content is expressed as:

$$\text{FAME} = \frac{\sum A - A_{C19}}{A_{C19}} \times \frac{W_{C19}}{W} \times 100 \quad (17)$$

where FAME represents the fatty acid methyl ester content in percent by mass (%(m/m)),  $\sum A$  is the total peak area from methyl ester  $C_{6:0}$  to methyl ester  $C_{24:1}$ ,  $A_{C19}$  is the peak area corresponding to methyl nanodecanoate ( $C_{19}$ ),  $W_{C19}$  is the weight, in milligrams (mg), of methyl nanodecanoate ( $C_{19}$ ), which is used as the internal standard, and  $W$  is the weight, in milligrams (mg), of the methyl ester produced in this study.

The glycerol and glyceride contents were identified based on the EN 14105:2011 standard method, as expressed by the following equations:

$$\text{Monoglycerides } (\%(\text{m/m})), M = \left( \frac{A_M}{A_{MC19}} \right) \times \left( \frac{M_{MC19}}{m} \right) \times 100 \quad (18)$$

$$\text{Diglycerides } (\%(\text{m/m})), D = \left( \frac{A_D}{A_{DC38}} \right) \times \left( \frac{M_{DC38}}{m} \right) \times 100 \quad (19)$$

$$\text{Triglycerides } (\%(\text{m/m})), T = \left( \frac{A_T}{A_{TC57}} \right) \times \left( \frac{M_{TC57}}{m} \right) \times 100 \quad (20)$$

$$\text{Free glycerol } (\%(\text{m/m})), G = \left[ a_G \left( \frac{A_G}{A_{EI1}} \right) + b_G \right] \times \left( \frac{M_{EI1}}{m} \right) \times 100 \quad (21)$$

$$\text{Total glycerol } (\%(\text{m/m})) = G + 0.255M + 0.146D + 0.103T \quad (22)$$

where  $A_M$ ,  $A_D$ , and  $A_T$  are the sum of the peak areas of the monoglycerides, diglycerides, and triglycerides respectively,  $A_{MC19}$  is the area of the internal standard monoglycerides  $C_{19}$ ,  $M_{MC19}$  is the weight, in milligrams (mg), of the internal standard monoglycerides  $C_{19}$ ,  $A_{DC38}$  is the peak area of internal standard  $C_{38}$ ,  $M_{DC38}$  is the weight, in milligrams (mg), of the internal standard

diglycerides  $C_{38}$ ,  $A_{TC57}$  is the area of the internal standard triglycerides  $C_{57}$ ,  $M_{TC57}$  is the weight, in milligrams (mg), of internal standard triglycerides  $C_{57}$ . In addition,  $m$  is the weight, in milligrams (mg), of the biodiesel sample,  $a_G$  and  $b_G$  are the regression coefficients of the calibration function of glycerol,  $A_G$  is the peak area of glycerol,  $A_{EI1}$  is the peak of internal standard 1,2,4-butanetriol, and  $M_{EI1}$  is the weight, in milligrams (mg), of the internal standard 1,2,4-butanetriol.

## 3. Results and discussion

### 3.1. Effect of reaction time on acid value

The effect of reaction time on acid value of the esterified *Ceiba pentandra* oil is shown in Fig. 4. It can be seen that the acid value is lowest (1.878 mg KOH/g) at a reaction time of 300 s. The presence of  $H_2SO_4$  catalyst at longer reaction times (300–360 s) results in a slow equilibrium reaction due to undesirable side reactions, which is evidenced by a slight increase in acid value. Ma et al. [46] found that microwave irradiation was able to convert 37%–78% of the free fatty acids (FFAs) whereas in this study, 69–88% of the FFAs were converted. Kim et al. [47] found that microwave irradiation improved the conversion of FFAs from 39.9% to 66.1%. Lieu et al. [48] undertook a kinetics study on microwave irradiation-assisted esterification of FFAs from CCPO. Their results showed range of acid values of the esterified *Ceiba pentandra* oil was 0.776–4.529 mg KOH/g. This indicates that microwave irradiation has the potential to reduce the FFAs in the esterified oil to the desired acid value (1.878 mg KOH/g).

### 3.2. ELM model

The ELM is a modeling technique used to predict and solve various types of engineering problems. It is a single-hidden-layer feedforward neural network where the parameters of the hidden layer are randomly generated [49]. The ELM can calculate the output weights analytically using the Moore-Penrose generalized inverse. Therefore, ELM is advantageous because of its breakneck learning speed and better generalization capability [15]. However, the main disadvantage of ELM is that it requires trial and error to determine the optimal ELM architecture. The trial-and-error procedure is very time-consuming and tedious. The randomness of the input weights can also reduce effectiveness of the algorithm and influences the algorithm performance such that the ELM output is not really stable [50–52]. The CPME yield values predicted by the ELM model for various combinations of transesterification process

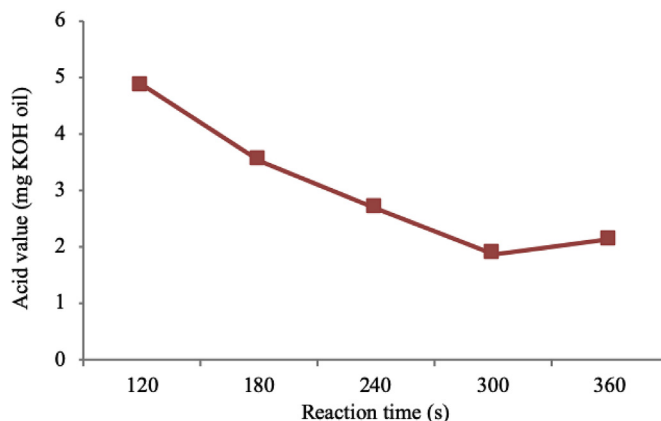


Fig. 4. Effect of reaction time on acid value of esterified *Ceiba pentandra* oil.

parameters are shown in Table 3. Fig. 5 shows the  $R$  values obtained by the ELM model for training, testing, and overall datasets are 0.999, 0.986, and 0.996 respectively. It can be seen the  $R$  values are all close to 1.000, indicating that there is good correlation between the experimental and predicted values. The  $R^2$  value and RMSE were 0.992 and 0.142 respectively, as shown in Table 2. The RMSE indicates the goodness of fit and it should be as low as possible because it represents the standard deviation of the residuals of the regression model [53]. Fig. 4 shows the comparison between the CPME yield values predicted by ELM model and those obtained from experiments. It can be observed ELM model is able to predict CPME yield remarkably well, indicating the former is a reliable method to predict the latter (see Fig. 6).

### 3.3. Random sub-sampling cross validation for ELM model

A total of 23 datasets were used for training while the remaining

six datasets were used for testing. The process was repeated ten times using various combinations of inputs with the same user-defined parameters, as shown in Table 4. Based on the results, the AAD and SD of the random sub-sampling cross validation are 0.00587 and 0.0026 respectively, indicating accuracy of the ELM model.

### 3.4. Optimization of transesterification process parameters

The optimum process parameters for microwave irradiation-assisted transesterification in order to maximize the CPME yield obtained from the ELM-CS model are as follows: (1) methanol/oil ratio: 60%, (2) KOH catalyst concentration: 0.84%(w/w), (3) stirring speed: 800 rpm, and (4) reaction time: 388 s. The corresponding optimal CPME yield predicted by the ELM-CS model is 96.19%. The optimum conditions predicted by the model were verified by carrying out three independent experimental replicates using the

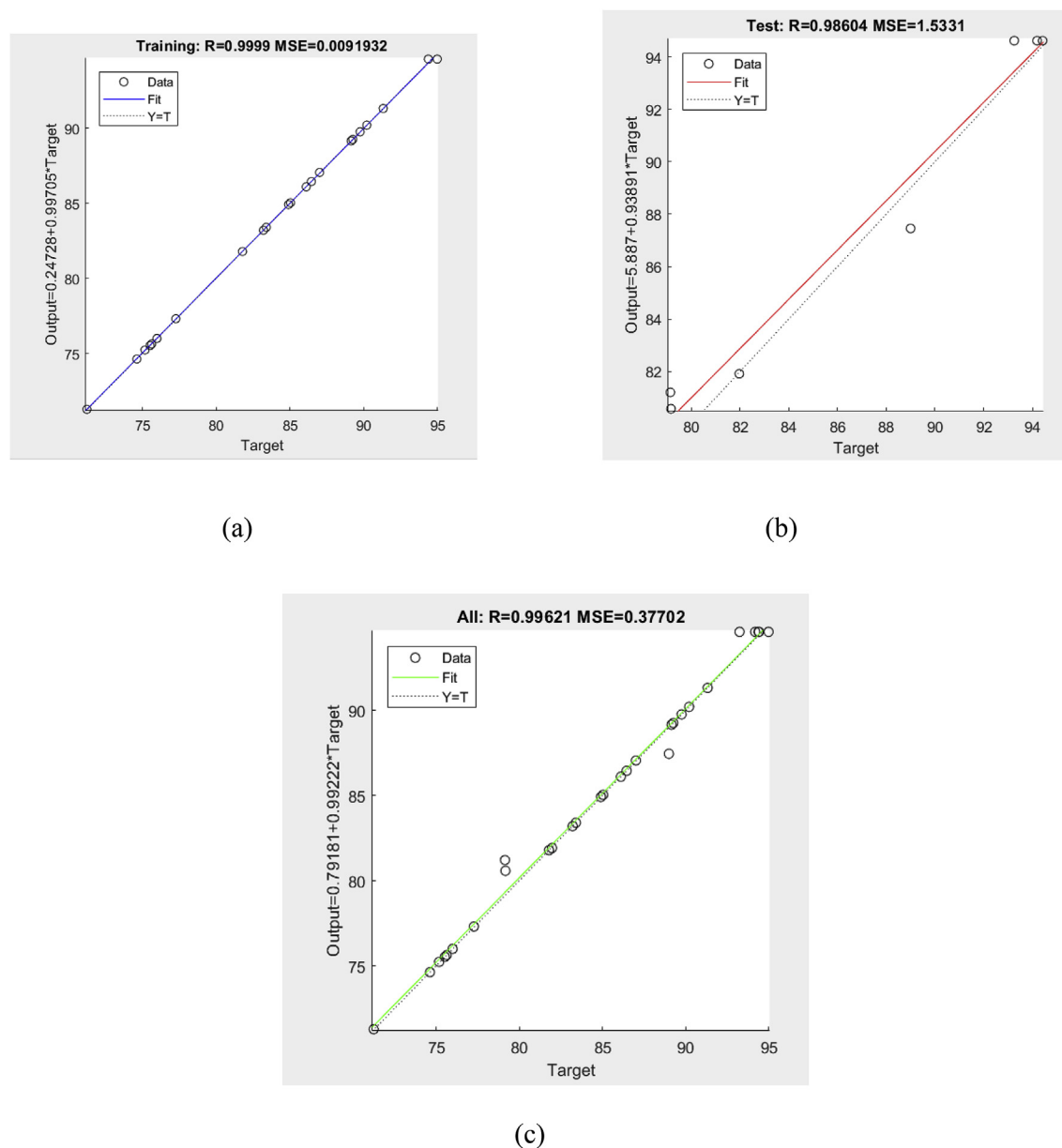


Fig. 5. Correlation between output and target values for (a) training dataset, (b) testing dataset, and (c) overall dataset.

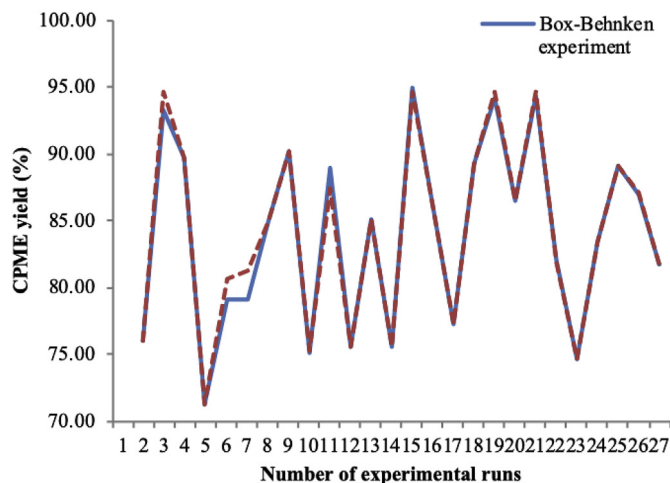


Fig. 6. Comparison of the CPME yield predicted by ELM model and CPME yield obtained from Box-Behnken experiment.

Table 4

Results of the random sub-sampling cross validation.

Repetition	AAD
Repeat 1	0.00455
Repeat 2	0.00512
Repeat 3	0.00500
Repeat 4	0.00320
Repeat 5	0.00551
Repeat 6	0.00363
Repeat 7	0.01280
Repeat 8	0.00713
Repeat 9	0.00703
Repeat 10	0.00477
Overall average	0.00587
SD	0.00260

optimum transesterification process parameters and average CPME yield was determined. The actual CPME yield obtained from the experiments using the microwave reactor is slightly lower, with a value of 95.42%. Since there is good agreement between the predicted and experimental CPME yield, this indicates that ELM model is capable of predicting the CPME yield with high accuracy.

### 3.5. Sensitivity analysis of the transesterification reaction parameters

Various combinations of inputs were used to determine the effect of each input parameter on the output of ELM model. Fig. 7 shows the level of significance of the input variables on the CPME yield. It can be observed the stirring speed has the most significant effect on CPME yield (25.62%), followed by reaction time (25.19%), and KOH catalyst concentration (25.05%). The methanol/oil ratio has the least significant effect, with a value of 24.15%.

### 3.6. Combined effects of the transesterification reaction parameters

Three-dimensional response surface plots were plotted in order to examine the combined effect of the transesterification process parameters on CPME yield, as shown in Fig. 8a–d. In general, CPME yield increases as the stirring speed, reaction time, KOH catalyst concentration, and methanol/oil ratio increase up to a certain value, and then decreases thereafter. Fig. 8a shows the combined effect of stirring speed and reaction time on CPME yield, and it can be seen

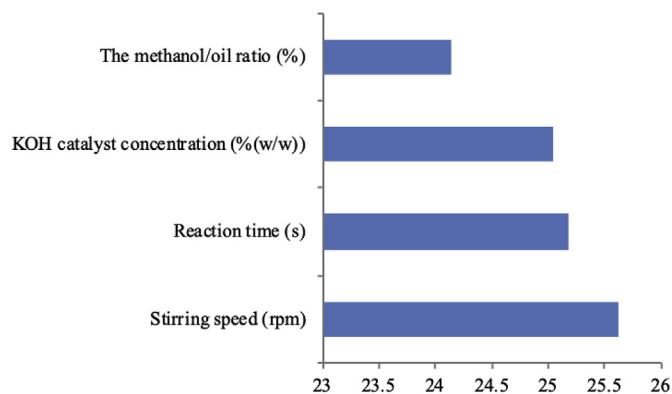


Fig. 7. Level of significance of input variables, indicating effect of each input variable on CPME yield.

that increasing the stirring speed and reaction time up to a certain point boosts it. The CPME yield is higher at higher stirring speeds and at longer reaction times. The highest CPME yield was 96.19%, obtained when the stirring speed and reaction time were 800 rpm and 388 s respectively. A higher stirring speed promotes the reaction between methanol and esterified oil which boosts CPME yield. Likewise, a longer reaction time ensures complete transesterification reaction, which boosts CPME yield. Fig. 8b shows the combined effects of reaction time and KOH catalyst concentration on CPME yield. The highest CPME yield was achieved when the reaction time and KOH catalyst concentration are 388 s and 0.84%(w/w) respectively. It can be observed the effect of KOH catalyst concentration was more pronounced at higher reaction times. This indicates the reactants (methanol, esterified *Ceiba pentandra* oil, and KOH catalyst) require a specific duration to ensure a homogeneous mixture, and which will increase CPME yield. This shows the reaction time and KOH catalyst concentration have a pronounced effect on the CPME yield. Fig. 8c shows the combined effect of KOH catalyst concentration and methanol/oil ratio on CPME yield. It can be seen CPME yield reaches its maximum when the methanol/oil ratio is within a range of 50–60%. A methanol/oil ratio of more than 60% has a moderate effect on CPME yield. It can be seen the KOH catalyst concentration determines CPME yield. The CPME yield slowly decreases when the KOH catalyst concentration increases beyond the optimal value of 0.84%(w/w). Hence, the KOH catalyst concentration is one of the important parameters that need to be controlled in order to attain a high CPME yield. High concentrations of KOH catalyst will result in emulsification and saponification of CPME during the purification process [54]. Fig. 8d shows combined effect of the stirring speed and methanol/oil ratio on CPME yield. The highest CPME yield (96.19%) was attained when the methanol/oil ratio and stirring speed were 60% and 800 rpm respectively. It is clear both stirring speed and methanol/oil ratio have a significant effect on the CPME yield. The CPME yield increases from 82.50% to 96.19% as the stirring speed increases from 600 rpm to 800 rpm. It is important to use the optimum stirring speed setting to ensure homogeneous mixing of methanol, KOH catalyst, and esterified *Ceiba pentandra* oil in order to achieve a complete transesterification process. In addition, it is important to ensure a suitable methanol/oil ratio in order to optimize the transesterification process. If the amount of methanol in the mixture is too low, this will produce more monoglycerides and diglycerides compared with methyl ester. In contrast, if the amount of methanol in the mixture is too high, this will lead to solubility of the by-product (glycerol) in the mixture, which will complicate the separation of methyl ester and by-

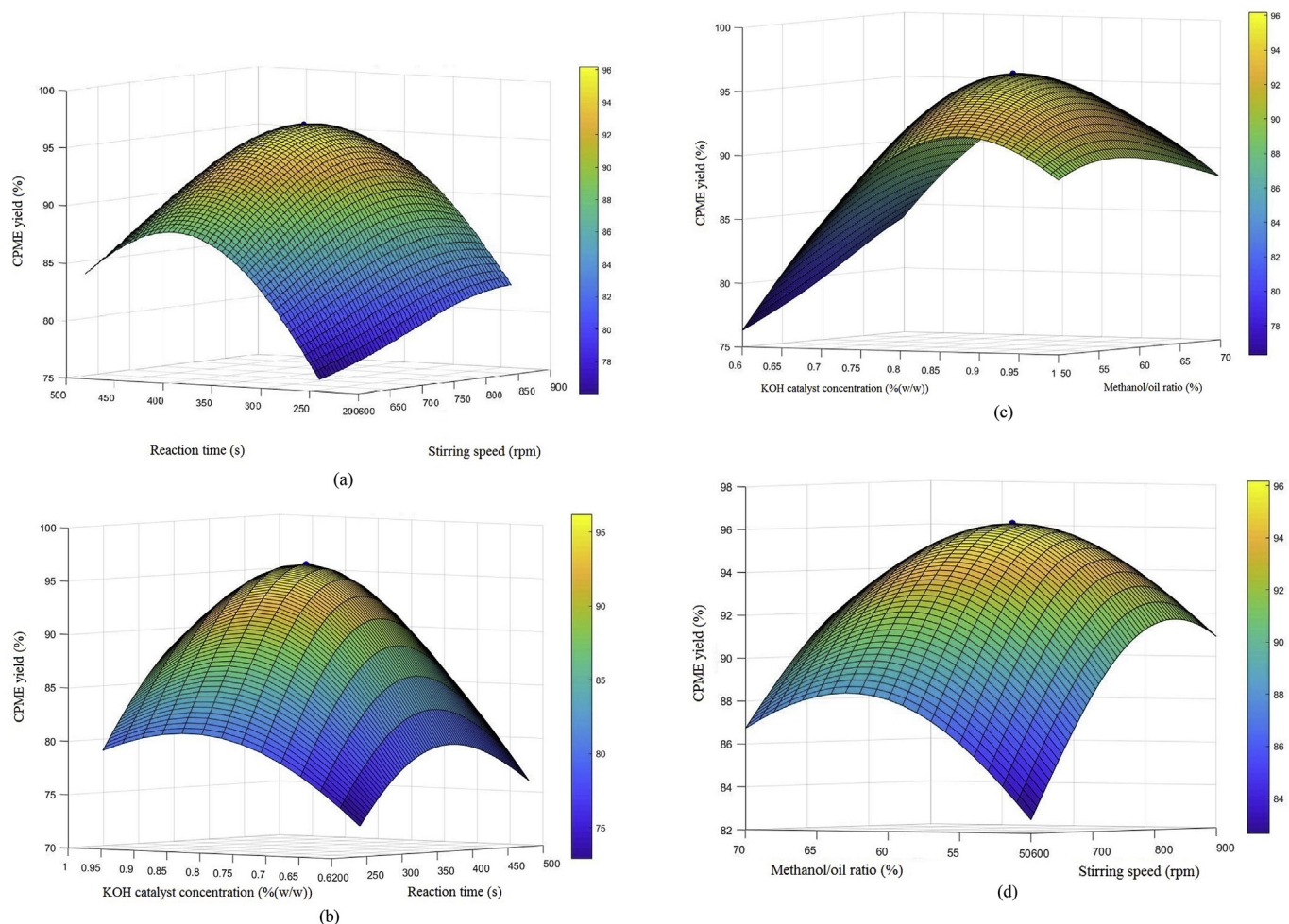


Fig. 8. (a–d) Three-dimensional response surface plots showing the combined effect of the transesterification process parameters on CPME yield.

product. It is crucial to use an appropriate amount of methanol because the microwave reactor is a closed system. Microwave irradiation-assisted transesterification does not allow excessive amounts of methanol in the transesterification process and therefore, the amount of methanol must be definite in order to boost CPME yield.

### 3.7. Model validation

In order to validate the prediction of optimal CPME yield, experiments were carried out in triplicate using the optimum microwave irradiation-assisted transesterification process parameters, and the results are summarized in Table 5. The average CPME yield is 95.42% with a standard deviation of 0.003. This indicates a very good agreement between the optimum CPME yield predicted by the ELM-CS model and the average CPME yield obtained from the experiments. Based on the results, it can be deduced the model is reliable and it is able to predict the optimal conditions of the microwave irradiation-assisted transesterification process.

### 3.8. Physicochemical properties of CCPO and CPME

The physicochemical properties of CCPO and CPME, such as kinematic viscosity at 40 °C, density at 15 °C, cloud point, pour point,

flash point, acid value, calorific value, oxidation stability, and FAME, glyceride, and glycerol contents were measured according to ASTM D6751 and EN 14214 standard test methods and the results are tabulated in Table 6. Kinematic viscosity is an important property of biodiesel and it is known that biodiesels have higher kinematic viscosities compared with diesel [55]. The kinematic viscosities of the CPME and CCPO were 18.74 and 4.69 mm<sup>2</sup>/s respectively, as seen in this study. The CPME has lower kinematic viscosity and acid value, higher heating value, and superior cold flow properties, indicating the advantages of producing biodiesel from *Ceiba pentandra* oil by microwave irradiation-assisted transesterification compared with conventional transesterification. It is well known acid values of both crude oil and methyl ester are influenced by the type of feedstock as well as the degree of refinement [56]. The high acid value of the CPME (0.18 mg KOH/g) is significantly reduced by acid-catalyzed esterification and indeed, it is proven that the CPME has the lowest acid value after acid-catalyzed esterification and alkaline-catalyzed transesterification. The flash point of the CPME is 158.5 °C, which is significantly higher than the flash point specified in the ASTM D6751 standard (130 °C). A higher flash point of CPME is desirable because this will reduce the risk of fire hazards, which is a primary concern when handling, transporting, and storing fuels [57]. However, the calorific value of CPME (40.276 MJ/kg) was higher in this study compared with those obtained by earlier researchers due to the composition of saturated and

**Table 5**  
CPME yield obtained from microwave irradiation-assisted transesterification process using the optimum process parameters.

Run	Reaction time (s)	KOH catalyst concentration (wt%)	Methanol/oil ratio (%)	Stirring speed (rpm)	CPME yield (%)
1	388	0.84	60	800	95.82
2	388	0.84	60	800	94.91
3	388	0.84	60	800	95.54
Average experimental CPME yield (%)					95.42
Predicted optimum CPME yield (%)					96.19
SD					0.003

**Table 6**  
Physicochemical properties of CCPO and CPME.

Properties	Unit	Standard test method	CCPO <sup>a</sup>	CPME <sup>a</sup>	CPME [7]	Diesel <sup>a</sup>
Density at 15 °C	kg/m <sup>3</sup>	D1298	906.5	883.6	875	826
Kinematic viscosity at 40 °C	mm <sup>2</sup> /s	D445	18.74	4.69	5.4	2.99
Flash point	°C	D93	186.5	158.5	156	72.5
Pour point	°C	D97	—	−2.0	—	−5
Cloud point	°C	D2500	—	−3.0	—	−8
Calorific value	MJ/kg	EN 14214	38.672	40.276	36.292	45.483
Copper strip corrosion	—	D130	—	1a	1a	1a
Oxidation stability	h	EN 14112	4.8	9.82	—	23.9
Acid value	mg KOH/g	D 664	16.2	0.18	—	0.06
FAME content	%(m/m)	EN 14103:2011	—	98.96	—	—
Monoglycerides	%(m/m)	EN14105	—	0.419	—	—
Diglycerides	%(m/m)	EN14105	—	0.108	—	—
Triglycerides	%(m/m)	EN14105	—	0.115	—	—
Free glycerol	%(m/m)	EN14105	—	0.017	—	—
Total glycerol	%(m/m)	EN14105	—	0.136	—	—

<sup>a</sup> Values measured in this study.

unsaturated fatty acids of CPME. The CPME has a relatively high oxidation stability (9.82 h), which is likely due to its higher amounts of saturated carbon chains which will increase the induction time of oxidation. Small amounts of unsaturated carbon chains will have a significant effect on oxidation stability [58,59]. In general, a high oxidation stability is favorable because this will reduce the likelihood of biodiesel to oxidize over an extended period. This property is essential for fuel storage and handling. Moreover, there is a high possibility the fuel will oxidize and deteriorate in the fuel tank and engine owing to high-temperature conditions and therefore, it is crucial for the fuel to have higher oxidation stability [58,60]. In addition, it is desirable for biodiesels to have higher oxidation stability because this will facilitate the supply and distribution of biodiesels to remote areas located far from biodiesel production facilities. The oxidation stability enhancement is likely due to the stearic and myristic fatty acid content of FAME [61]. Biodiesel consists of ester molecules, which tend to hydrolyze into alcohol and acid in the presence of air or oxygen [62]. The presence of alcohol reduces the flash point whereas the presence of acid increases its (acid) value [63]. In contrast, a higher polyunsaturated fatty acid content will improve the cold flow properties, but the resultant biodiesel is more susceptible to oxidation [64,65]. The FAME of CPME obtained in this study was 98.96%(m/m), which indicates the biodiesel produced is of very high quality. The monoglycerides, diglycerides, and triglycerides found in CPME were 0.42, 0.11, and 0.11% (m/m) respectively, which are below permissible limits of 0.8, 0.2, and 0.2%(m/m) respectively. Total glycerol found in the methyl ester was 0.14, which was below the permissible limit of 0.25. Results showed microwave irradiation had successfully reduced the amounts of monoglycerides, diglycerides, and triglycerides to acceptable levels. This indicate that microwave irradiation is able to enhance the conversion of methyl ester and minimize the concentrations of glycerides and glycerol.

### 3.9. FTIR spectrum of the CPME

The functional groups of the CPME were determined using FTIR spectroscopy. Fig. 9 shows the FTIR spectrum of the CPME, which provides insight on the oil-to-methyl ester conversion process. The FTIR spectrum shows the wavenumber at which the absorption peak occurs, functional group, type of vibration, and absorption intensity. It can be inferred from FTIR spectrum CPME is composed of long-chain FAMES. There are three bands attributed to the bonds in COOH functional group, indicating the presence of carboxylates. The peaks at 2986, 2923, and 2853 cm<sup>−1</sup> correspond to C–H, vinylic/olefinic (C–H) and alcohol group (OH, H-bond) respectively. The peaks at 1169–1566 cm<sup>−1</sup> correspond to the bending vibrations of the methyl, methylene hydrocarbon, and unsaturated C–C bonds respectively. The peak at 858 cm<sup>−1</sup> indicates shear vibration of C–O whereas the peak at 720 cm<sup>−1</sup> indicates rocking-bending vibration of the methylene group. The characteristic peak at 1724 cm<sup>−1</sup> with strong absorption intensity is ascribed to the carbonyl group of methyl ester (–CO–OCH<sub>3</sub>). The results indicate CPME synthesis is successful.

### 3.10. Advantages and disadvantages of microwave irradiation

Microwave irradiation is a well-established method of accelerating and enhancing chemical reactions because it delivers the energy directly to the reactants [66]. Therefore, heat transfer is more effective than conventional heating and its reaction time is much shorter, lower oil/methanol ratio, and less energy consumption. Microwave irradiation accelerates the reaction and makes the separation process easier compared with conventional heating [34]. The optimum parameters of the microwave irradiation-assisted transesterification process conditions obtained are as follows: (1) methanol/oil ratio: 60%, (2) KOH catalyst concentration: 0.84%(w/w), (3) stirring speed: 800 rpm, and (4)

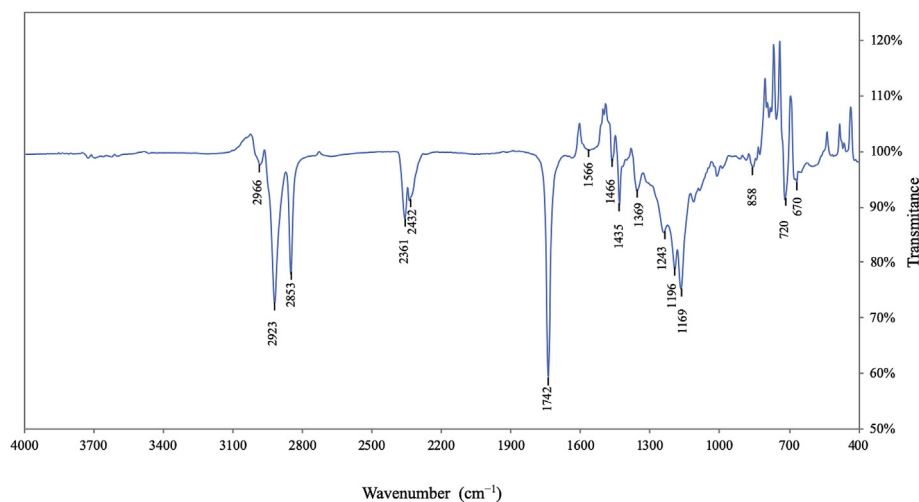


Fig. 9. FTIR spectrum of the CPME.

reaction time: 388 s. The corresponding CPME yield is 96.19%. Three independent experiments were conducted using the optimum process parameters and the average biodiesel yield is found to be 95.42%. The reaction time of 388 s in this study was significantly shorter than that of Ponappa et al. [67], who optimized biodiesel production from *Ceiba pentandra* oil (kapok seed oil) using response surface methodology assisted by ultrasonic energy, where the reaction time was 32.17 min. Kusumo et al. [7] optimized the transesterification process of *Ceiba pentandra* oil using kernel-based extreme learning machine and artificial neural networks and the time required to complete the reaction was 108 min. The microwave method requires a lower concentration of catalyst (0.84%(w/w)) compared with the ultrasound method (1.55%(w/w)) and conventional transesterification (1%(w/w)). However, the main disadvantage of microwave technology is uncontrolled heating due to poor understanding of the occurrence of dielectric phenomenon. In addition, there are safety issues concerning the use of microwave technology for biodiesel production, which makes it difficult to scale-up microwave irradiation-assisted transesterification for industrial production [68,69].

#### 4. Conclusion

In this study, *Ceiba pentandra* methyl ester was produced from microwave irradiation-assisted transesterification. The microwave reactor is suitable for small-scale synthesis of biodiesel which minimizes wastage of crude oil because the maximum allowable volume in the glass vial is 10–20 mL compared with a conventional heating reactor. An ELM-CS model was developed to optimize the transesterification process parameters in order to boost CPME yield. The predicted CPME yield was found to be 96.19%, which showed very good agreement of the experiments (95.42%). Box-Behnken design was used to obtain the best combination of methanol/oil ratio (60%), KOH catalyst concentration (0.84%(w/w)), reaction time (388 s), and stirring speed (800 rpm). The FAME of the CPME was 98.96%, which indicates high purity of methyl ester produced in this study. In addition, oxidation stability increased by twofold after the transesterification process and based on the cold flow properties, it can be deduced that the CPME can be used in cold climate countries. Statistical analysis was then conducted to verify the accuracy of ELM-CS model and the results showed the model is reliable to predict the optimal parameters for microwave irradiation-assisted transesterification, based on the high  $R$  (0.996)

and  $R^2$  (0.992) values as well as low RMSE (0.142). In general, the ELM-CS model is capable of predicting the optimum process parameters in order to maximize CPME yield while minimizing overall biodiesel production cost associated with conventional trial and error experimental techniques. Based on the results obtained from the ELM-CS model, the optimum process parameters can be used for microwave irradiation-assisted transesterification regardless of the feedstock, producing biodiesels that fulfill the physicochemical properties stipulated in the ASTM D6751 and EN 14214 standards.

#### Acknowledgments

This research was supported by the Direktorat Jenderal Penguatan Riset dan Pengembangan Kementerian Riset, Teknologi dan Pendidikan Tinggi Republik Indonesia, (Grant no. 147/SP2H/LT/DRPM/2019) and Politeknik Negeri Medan, Medan, Indonesia. It also received the financial support of AAIBE Chair of Renewable Energy (Grant no: 201801 KETTHA), and Universiti Tenaga Nasional Internal Grant (UNIIG 2017) (Grant no.: J510050691). The authors express their appreciation to Ministry of Education Malaysia and University of Malaya, Kuala Lumpur Malaysia, for funding this work under their FRGS-MRSA (MO014-2016).

#### Appendix A. Supplementary data

Supplementary data to this article can be found online at <https://doi.org/10.1016/j.renene.2019.07.065>.

#### References

- [1] M. Faried, M. Samer, E. Abdelsalam, R.S. Yousef, Y.A. Attia, A.S. Ali, Biodiesel production from microalgae: processes, technologies and recent advancements, *Renew. Sustain. Energy Rev.* 79 (2017) 893–913.
- [2] S. Dharma, H.C. Ong, H.H. Masjuki, A.H. Sebayang, A.S. Silitonga, An overview of engine durability and compatibility using biodiesel–bioethanol–diesel blends in compression-ignition engines, *Energy Convers. Manag.* 128 (2016) 66–81.
- [3] W.N.M. Wan Ghazali, R. Mamat, H.H. Masjuki, G. Najafi, Effects of biodiesel from different feedstocks on engine performance and emissions: a review, *Renew. Sustain. Energy Rev.* 51 (2015) 585–602.
- [4] M. Shahabuddin, A.M. Liaquat, H.H. Masjuki, M.A. Kalam, M. Mofijur, Ignition delay, combustion and emission characteristics of diesel engine fueled with biodiesel, *Renew. Sustain. Energy Rev.* 21 (2013) 623–632.
- [5] J. Gupta, M. Agarwal, A.K. Dalai, Optimization of biodiesel production from mixture of edible and nonedible vegetable oils, *Biocatal. Agric. Biotechnol.* 8 (2016) 112–120.

- [6] A. Woinaroschy, Multiobjective optimal design for biodiesel sustainable production, *Fuel* 135 (2014) 393–405.
- [7] F. Kusumo, A.S. Silitonga, H.H. Masjuki, H.C. Ong, J. Siswanto, T.M.I. Mahlia, Optimization of transesterification process for Ceiba pentandra oil: a comparative study between kernel-based extreme learning machine and artificial neural networks, *Energy* 134 (2017) 24–34.
- [8] S. Dharma, M.H. Hassan, H.C. Ong, A.H. Sebayang, A.S. Silitonga, F. Kusumo, J. Milano, Experimental study and prediction of the performance and exhaust emissions of mixed *Jatropha curcas*–*Ceiba pentandra* biodiesel blends in diesel engine using artificial neural networks, *J. Clean. Prod.* 164 (2017) 618–633.
- [9] A.H. Sebayang, H.H. Masjuki, H.C. Ong, S. Dharma, A.S. Silitonga, F. Kusumo, J. Milano, Optimization of bioethanol production from sorghum grains using artificial neural networks integrated with ant colony, *Ind. Crops Prod.* 97 (2017) 146–155.
- [10] E. Betiku, S.S. Okunsolawo, S.O. Ajala, O.S. Odedele, Performance evaluation of artificial neural network coupled with generic algorithm and response surface methodology in modeling and optimization of biodiesel production process parameters from shea tree (*Vitellaria paradoxa*) nut butter, *Renew. Energy* 76 (2015) 408–417.
- [11] G.R. Moradi, S. Dehghani, F. Khosravian, A. Arjmandzadeh, The optimized operational conditions for biodiesel production from soybean oil and application of artificial neural networks for estimation of the biodiesel yield, *Renew. Energy* 50 (2013) 915–920.
- [12] M.S. Ismail, M. Moghavvemi, T. Mahlia, Genetic algorithm based optimization on modeling and design of hybrid renewable energy systems, *Energy Convers. Manag.* 85 (2014) 120–130.
- [13] H.C. Ong, H. Masjuki, T. Mahlia, A. Silitonga, W. Chong, K. Leong, Optimization of biodiesel production and engine performance from high free fatty acid Calophyllum inophyllum oil in CI diesel engine, *Energy Convers. Manag.* 81 (2014) 30–40.
- [14] A.H. Sebayang, H.H. Masjuki, H.C. Ong, S. Dharma, A.S. Silitonga, F. Kusumo, J. Milano, Prediction of engine performance and emissions with Manihot glaziovii bioethanol – Gasoline blended using extreme learning machine, *Fuel* 210 (2017) 914–921.
- [15] K.I. Wong, P.K. Wong, C.S. Cheung, C.M. Vong, Modeling and optimization of biodiesel engine performance using advanced machine learning methods, *Energy* 55 (2013) 519–528.
- [16] S. Dharma, H.H. Masjuki, H.C. Ong, A.H. Sebayang, A.S. Silitonga, F. Kusumo, T.M.I. Mahlia, Optimization of biodiesel production process for mixed *Jatropha curcas*–*Ceiba pentandra* biodiesel using response surface methodology, *Energy Convers. Manag.* 115 (2016) 178–190.
- [17] N. Damani, H.C. Ong, W. Chong, A. Silitonga, Biodiesel Production from Calophyllum Inophyllum – Palm Mixed Oil, *Energy Sources, Part A: Recovery, Utilization, and Environmental Effects*, 2017, pp. 1–7.
- [18] F. Kusumo, A. Silitonga, H.C. Ong, H. Masjuki, T. Mahlia, A Comparative Study of Ultrasound and Infrared Transesterification of Sterculia Foetida Oil for Biodiesel Production, *Energy Sources, Part A: Recovery, Utilization, and Environmental Effects*, 2017, pp. 1–8.
- [19] L.F. Chuah, J.J. Klemeš, S. Yusup, A. Bokhari, M.M. Akbar, A review of cleaner intensification technologies in biodiesel production, *J. Clean. Prod.* 146 (2017) 181–193.
- [20] L. Dehghan, M.-T. Golmakani, S.M.H. Hosseini, Optimization of microwave-assisted accelerated transesterification of inedible olive oil for biodiesel production, *Renew. Energy* 138 (2019) 915–922.
- [21] M.G. Nayak, A.P. Vyas, Optimization of microwave-assisted biodiesel production from Papaya oil using response surface methodology, *Renew. Energy* 138 (2019) 18–28.
- [22] A. Silitonga, H. Masjuki, T. Mahlia, H. Ong, A. Atabani, W. Chong, A global comparative review of biodiesel production from *Jatropha curcas* using different homogeneous acid and alkaline catalysts: study of physical and chemical properties, *Renew. Sustain. Energy Rev.* 24 (2013) 514–533.
- [23] P. Verma, M.P. Sharma, Review of process parameters for biodiesel production from different feedstocks, *Renew. Sustain. Energy Rev.* 62 (2016) 1063–1071.
- [24] S. Budžaki, G. Miljić, M. Tišma, S. Sundaram, V. Hessel, Is there a future for enzymatic biodiesel industrial production in microreactors? *Appl. Energy* 201 (2017) 124–134.
- [25] W. Yang, J.F. Casey, Y. Gao, A new sample preparation method for crude or fuel oils by mineralization utilizing single reaction chamber microwave for broader multi-element analysis by ICP techniques, *Fuel* 206 (2017) 64–79.
- [26] J.-Z. Liu, Q. Cui, Y.-F. Kang, Y. Meng, M.-Z. Gao, T. Efferth, Y.-J. Fu, *Euonymus maackii* Rupr seed oil as a new potential non-edible feedstock for biodiesel, *Renew. Energy* 133 (2019) 261–267.
- [27] N. Azcan, O. Yılmaz, Microwave assisted transesterification of waste frying oil and concentrate methyl ester content of biodiesel by molecular distillation, *Fuel* 104 (2013) 614–619.
- [28] A.R. Gupta, V.K. Rathod, Calcium diglyceride catalyzed biodiesel production from waste cooking oil in the presence of microwave: optimization and kinetic studies, *Renew. Energy* 121 (2018) 757–767.
- [29] T. Chee Loong, A. Idris, One step transesterification of biodiesel production using simultaneous cooling and microwave heating, *J. Clean. Prod.* 146 (2017) 57–62.
- [30] I. Choedkiatsakul, K. Ngaosuwan, S. Assabumrungrat, S. Mantegna, G. Cravotto, Biodiesel production in a novel continuous flow microwave reactor, *Renew. Energy* 83 (2015) 25–29.
- [31] Y.K. Walia, K. Kishore, D. Vasu, G. DK, Physico-chemical analysis of Ceiba pentandra (kapok), *Int. J. Circuit Theory Appl. Sci.* 1 (2009) 15–18.
- [32] A.E. Atabani, A.S. Silitonga, I.A. Badruddin, T.M.I. Mahlia, H.H. Masjuki, S. Mekhilef, A comprehensive review on biodiesel as an alternative energy resource and its characteristics, *Renew. Sustain. Energy Rev.* 16 (2012) 2070–2093.
- [33] A.S. Silitonga, H.H. Masjuki, T.M.I. Mahlia, H.C. Ong, W.T. Chong, M.H. Boosroh, Overview properties of biodiesel diesel blends from edible and non-edible feedstock, *Renew. Sustain. Energy Rev.* 22 (2013) 346–360.
- [34] J. Milano, H.C. Ong, H.H. Masjuki, A.S. Silitonga, W.-H. Chen, F. Kusumo, S. Dharma, A.H. Sebayang, Optimization of biodiesel production by microwave irradiation-assisted transesterification for waste cooking oil-Calophyllum inophyllum oil via response surface methodology, *Energy Convers. Manag.* 158 (2018) 400–415.
- [35] L.A. Jermolovicus, L.C.M. Cantagesso, R.B. do Nascimento, E.R. de Castro, E.V. dos, S. Pouzada, J.T. Senise, Microwave fast-tracking biodiesel production, *Chem. Eng. Process: Process Intensification* 122 (2017) 380–388.
- [36] S.A. El Sherbiny, A.A. Refaat, S.T. El Sheltawy, Production of biodiesel using the microwave technique, *J. Adv. Res.* 1 (2010) 309–314.
- [37] P. Kundu, V. Paul, V. Kumar, I.M. Mishra, Formulation development, modeling and optimization of emulsification process using evolving RSM coupled hybrid ANN-GA framework, *Chem. Eng. Res. Des.* 104 (2015) 773–790.
- [38] S. Wu, Y. Wang, S. Cheng, Extreme learning machine based wind speed estimation and sensorless control for wind turbine power generation system, *Neurocomputing* 102 (2013) 163–175.
- [39] K.I. Wong, C.M. Vong, P.K. Wong, J. Luo, Sparse Bayesian extreme learning machine and its application to biofuel engine performance prediction, *Neurocomputing* 149 (2015) 397–404.
- [40] A.S. Joshi, O. Kulkarni, G.M. Kakandikar, V.M. Nandedkar, Cuckoo search optimization – a review, *Mater. Today: Proceedings* 4 (2017) 7262–7269.
- [41] X.-S. Yang, Nature-Inspired Meta-Heuristic Algorithms, *Univer Press*, 2010.
- [42] X.-S. Yang, S. Deb, Engineering optimisation by cuckoo search, *Int. J. Math. Model. Numer. Optim.* 1 (2010) 330–343.
- [43] C. Bindhu, J.R.C. Reddy, B.V.S.K. Rao, T. Ravinder, P.P. Chakrabarti, M.S.L. Karuna, R.B.N. Prasad, Preparation and evaluation of biodiesel from *Sterculia foetida* seed oil, *J. Am. Oil Chem. Soc.* 89 (2012) 891–896.
- [44] P. Shivakumar, Pai Srinivasa, B.R. Shrinivasa Rao, Artificial Neural Network based prediction of performance and emission characteristics of a variable compression ratio CI engine using WCO as a biodiesel at different injection timings, *Appl. Energy* 88 (2011) 2344–2354.
- [45] D.M. Hamby, A review of techniques for parameter sensitivity analysis of environmental models, *Environ. Monit. Assess.* 32 (1994) 135–154.
- [46] L. Ma, E. Lv, L. Du, J. Lu, J. Ding, Statistical modeling/optimization and process intensification of microwave-assisted acidified oil esterification, *Energy Convers. Manag.* 122 (2016) 411–418.
- [47] D. Kim, J. Choi, G.-J. Kim, S.K. Seol, S. Jung, Accelerated esterification of free fatty acid using pulsed microwaves, *Bioresour. Technol.* 102 (2011) 7229–7231.
- [48] T. Lieu, S. Yusup, M. Moniruzzaman, Kinetic study on microwave-assisted esterification of free fatty acids derived from Ceiba pentandra Seed Oil, *Bioresour. Technol.* 211 (2016) 248–256.
- [49] G.-B. Huang, Q.-Y. Zhu, C.-K. Siew, Extreme learning machine: theory and applications, *Neurocomputing* 70 (2006) 489–501.
- [50] V. Kadiramanathan, S. Fabri, Stable nonlinear adaptive control with growing radial basis function networks, *IFAC Proc. Vol.* 28 (1995) 245–250.
- [51] Y. Lu, N. Sundararajan, P. Saratchandran, Performance evaluation of a sequential minimal radial basis function (RBF) neural network learning algorithm, *IEEE Trans. Neural Netw.* 9 (1998) 308–318.
- [52] X. Wang, M. Han, Improved extreme learning machine for multivariate time series online sequential prediction, *Eng. Appl. Artif. Intell.* 40 (2015) 28–36.
- [53] N.B. Ishola, O.O. Adeyemi, A.J. Adesina, V.O. Odude, O.O. Oyetunde, A.A. Okeleye, A.R. Soji-Adekunle, E. Betiku, Adaptive neuro-fuzzy inference system-genetic algorithm vs. response surface methodology: a case of optimization of ferric sulfate-catalyzed esterification of palm kernel oil, *Process Saf. Environ. Prot.* 111 (2017) 211–220.
- [54] J. Milano, H.C. Ong, H.H. Masjuki, A.S. Silitonga, F. Kusumo, S. Dharma, A.H. Sebayang, M.Y. Cheah, C.-T. Wang, Physicochemical property enhancement of biodiesel synthesis from hybrid feedstocks of waste cooking vegetable oil and Beauty leaf oil through optimized alkaline-catalysed transesterification, *Waste Manag.* 80 (2018) 435–449.
- [55] G. Knothe, L.F. Razon, Biodiesel fuels, *Prog. Energy Combust. Sci.* 58 (2017) 36–59.
- [56] G. Knothe, Chapter 2 - biodiesel and its properties A2 - McKee, Thomas A, in: D.G. Hayes, D.F. Hildebrand, R.J. Weselake (Eds.), *Industrial Oil Crops*, AOCs Press, 2016, pp. 15–42.
- [57] P. Tamilselvan, N. Nallusamy, S. Rajkumar, A comprehensive review on performance, combustion and emission characteristics of biodiesel fuelled diesel engines, *Renew. Sustain. Energy Rev.* 79 (2017) 1134–1159.
- [58] J. Pullen, K. Saeed, An overview of biodiesel oxidation stability, *Renew. Sustain. Energy Rev.* 16 (2012) 5924–5950.
- [59] D.-S. Kim, H.-S. Kim, K.-T. Lee, D.-L. Hong, S.-R. Cho, J.H. Pan, Y.B. Park, Y.-B. Lee, J.K. Kim, E.-C. Shin, Chemical characterization and oxidative stability of medium- and long-chain fatty acid profiles in tree-borne seed oils, *J. Anal. Methods Chem.* 2018 (2018) 9 (2018) 2178684–2178684.
- [60] N. Kumar, Oxidative stability of biodiesel: causes, effects and prevention, *Fuel* 190 (2017) 328–350.

- [61] S.K. Hoekman, A. Broch, C. Robbins, E. Ceniceros, M. Natarajan, Review of biodiesel composition, properties, and specifications, *Renew. Sustain. Energy Rev.* 16 (2012) 143–169.
- [62] E.C. Zuleta, L. Baena, L.A. Rios, J.A. Calderón, The oxidative stability of biodiesel and its impact on the deterioration of metallic and polymeric materials: a review, *J. Braz. Chem. Soc.* 23 (2012) 2159–2175.
- [63] I.A. Musa, The effects of alcohol to oil molar ratios and the type of alcohol on biodiesel production using transesterification process, *Egypt. J. Petrol.* 25 (2016) 21–31.
- [64] L.M.d.S. Freire, I.M.G.d. Santos, J.R. de Carvalho Filho, A.M.T.d.M. Cordeiro, L.E.B. Soledade, V.J. Fernandes, A.S. de Araujo, A.G. de Souza, Influence of the synthesis process on the properties of flow and oxidative stability of biodiesel from *Jatropha curcas* biodiesel, *Fuel* 94 (2012) 313–316.
- [65] I.M. Monirul, H.H. Masjuki, M.A. Kalam, N.W.M. Zulkifli, H.K. Rashedul, M.M. Rashed, H.K. Imdadul, M.H. Mosarof, A comprehensive review on biodiesel cold flow properties and oxidation stability along with their improvement processes, *RSC Adv.* 5 (2015) 86631–86655.
- [66] F. Motasemi, F.N. Ani, A review on microwave-assisted production of biodiesel, *Renew. Sustain. Energy Rev.* 16 (2012) 4719–4733.
- [67] K. Ponappa, V. Velmurugan, P.A. Franco, T.R. Kannan, R. Ragurajan, Optimization of biodiesel production from *Ceiba Pentandra* (kapok seed oil) using response surface methodology assisted by ultrasonic energy method, *Int. J. Chemtech Res.* 9 (2016) 794–803.
- [68] A. Mazubert, M. Poux, J. Aubin, Intensified processes for FAME production from waste cooking oil: a technological review, *Chem. Eng. J.* 233 (2013) 201–223.
- [69] L. Buchori, I. Istadi, P. Purwanto, Advanced chemical reactor technologies for biodiesel production from vegetable oils - a review, *Bull. Chem. React. Eng. Catal.* 11 (2016) 406–430.